CBN 00-2

Transfer Map of an RF Cavity in a Solenoid Field with Steering Magnets

Daniel B. Fromowitz

Wilson Lab, Cornell University, Ithaca, NY 14853, USA
(e-mail: dbf5@cornell.edu)
January 13, 2000

The derivation of a transfer map for an RF cavity in a solenoid field with steerings is presented. This map has been incorporated into the BMAD *software [1] so that CESR linac cavities may be simulated.*

1 Introduction

In order to model the CESR linac injection system, transfer map routines were created to simulate the optics that appear in a linac. These optics are different than those found in a storage ring. The new routines deal correctly with the low energy and large transverse momentum that may appear in the linac.

In the linac, steerings coils are wrapped around the RF cavities. Some of the cavities are also enclosed in a long solenoid. In contrast to storage ring cavities, the beam energy dramatically increases in the linac cavities. This means that the effect of the steerings (kickers) depends upon the position along the cavity length.

The new routines have been written into the *BMAD* software. The routines (1) superimpose an RF cavity, a solenoid, and steerings, (2) correctly treat the changing energy within a cavity, (3) account for the changing transverse momentum within a cavity, (4) and do not assume the transverse momentum is small (most significant shortly after the positron converter solenoid).

The specifics of the algebra in determining the transfer maps is very tedious. Therefore, only the basic steps are presented in this paper. For a detailed look at the mathematics involved, see reference [2].

Note that this derivation ignores wake fields and space charge effects, as do the original *BMAD* routines.

2 Energy Increase

The RF in the cavity changes the energy of the beam. We first assume that the phase of RF that a given particle sees throughout the cavity is [3]

$$\phi(s) = \omega \int_0^s \frac{ds'}{v_s(s')} - \omega t(s) \tag{1}$$

where ω is the RF frequency, v_s is the longitudinal speed of the particle, and t is the time as a function of the position s. Assuming the speed is constant and the longitudinal displacement is roughly constant, the phase may be rewritten as

$$\phi(s) = \frac{\omega z(0)}{v_s(0)} + \phi_0 \tag{2}$$

where ϕ_0 is an overall phase (applies to every particle), z is the longitudinal displacement, and the "0" argument refers to initial values.

The effective electric potential V seen by the particle is

$$V \equiv V_0 \sin(\phi(s)) \tag{3}$$

where V_0 is the maximum potential that may be seen. The energy $U(s)$ at a given point along the cavity is

$$U(s) = U(0) + \frac{qVs}{L} \tag{4}$$

where $U(0)$ is the initial energy, s is the position along the section measured from the upstream end, and L is the total section length. In accelerator energy units,

$$\delta(s) = \delta(0) + \frac{qVs}{LU_0} \tag{5}$$

where U_0 is the beam design energy.

3 Longitudinal Displacement

Because the beam will not be extremely relativistic soon after creation, the longitudinal displacement z does not have the same meaning as it does in a storage ring. In a storage ring, z is constant except in bending magnets. In the linac, the longitudinal displacement generally increases in magnitude. The longitudinal displacement in the linac will be defined relative to a hypothetical particle traveling at c (a luxon) and starting at the point of positron creation. The longitudinal displacement of a particle when the luxon reaches a distance L is

$$z(L) = z(0) + s - L \tag{6}$$

where s is the actual distance traveled by the charged particle. The trick is to calculate s.

The time elapsed t_{total} for the luxon to cross the section is L/c. However, this is necessarily the same time for the charged particle to travel the distance s. Express this time as

$$t_{\text{total}} = \int_{\gamma(0)}^{\gamma(s)} \frac{d\gamma}{\dot{\gamma}}. \tag{7}$$

Using special relativity ($U = \gamma m_e c^2$) and the electric field ($E = V/L$), Equation 4 becomes

$$\gamma(s) = \gamma(0) + \frac{|q|\, Es}{m_e c^2} \tag{8}$$

where the absolute value was inserted because, like regular *BMAD* RF cavities, the RF is assumed to always be accelerating, given proper phasing. Define a new electric constant

$$C_E \equiv \frac{|q|\, E}{m_e c^2} \tag{9}$$

so that

$$\gamma(s) = \gamma(0) + C_E\, s. \tag{10}$$

Use

$$\dot{\gamma} = c\, C_E \sqrt{1 - \frac{1}{\gamma^2}} \tag{11}$$

and the previous equations to get

$$z(L) = z(0) + \frac{\sqrt{1 + \left(C_E L + \sqrt{\gamma_0^2 - 1}\right)^2} - \gamma_0}{C_E} - L. \tag{12}$$

In a storage ring, where C_E would be small and γ is always high, we would find that the equation reduces to $z(L) = z(0)$.

4 The Fringe Fields

Before entering or after leaving the uniform part of the field of a solenoid, the particle must pass through a fringe field. It is assumed that there is no longitudinal acceleration present in the region of the fringe and that no steerings distort the fringe. The rotational symmetry implies that canonical angular momentum is conserved [3]. Using the approximation that the fringe field is infinitesimally thin, then the angular velocity of the particle $\dot{\theta}(0)$ just after crossing the beginning fringe is related to the angular velocity $\dot{\theta}_b$ just *before* the fringe by

$$\dot{\theta}(0) = \dot{\theta}_b - \frac{qB_s}{2\gamma_b m_e}. \tag{13}$$

where B_s is the full value of the solenoid field and is positive if the field points downstream. The angular velocity $\dot{\theta}_a$ just *after* crossing the ending fringe is related to the angular velocity $\dot{\theta}(L)$ before crossing this fringe by

$$\dot{\theta}_a = \dot{\theta}(L) + \frac{qB_s}{2\gamma_a m_e}. \tag{14}$$

These values must be converted into accelerator units. Use relations such as $\dot{\theta} = \theta' \dot{s}$ and

$$\dot{s}\gamma = c\sqrt{\frac{\gamma^2 - 1}{1 + x'^2 + y'^2}}. \tag{15}$$

to get accelerator unit equations such as

$$x'(0) = x'_b + y_b \frac{C_M}{2}\sqrt{\frac{1 + x_b'^2 + y_b'^2}{\gamma_b^2 - 1}} \tag{16}$$

with the new, magnetic constant defined by

$$C_M \equiv \frac{qB_s}{m_e c}. \tag{17}$$

We can now determine the transfer matrix for the first fringe $M_{\rm 1st.\ fr}$ and for the second fringe $M_{\rm 2nd.\ fr}$:

$$\begin{bmatrix} x(0) \\ x'(0) \\ y(0) \\ y'(0) \end{bmatrix} = M_{\rm 1st\ fr} \begin{bmatrix} x_b \\ x'_b \\ y_b \\ y'_b \end{bmatrix} \tag{18}$$

with

$$M_{\rm 1st\ fr} = \begin{bmatrix} 1 & 0 & 0 & 0 \\ 0 & 1 & \frac{C_M}{2}\sqrt{\frac{1+x_b'^{\,2}+y_b'^{\,2}}{\gamma_b^2-1}} & 0 \\ 0 & 0 & 1 & 0 \\ -\frac{C_M}{2}\sqrt{\frac{1+x_b'^{\,2}+y_b'^{\,2}}{\gamma_b^2-1}} & 0 & 0 & 1 \end{bmatrix} \tag{19}$$

and

$$\begin{bmatrix} x_a \\ x'_a \\ y_a \\ y'_a \end{bmatrix} = M_{\rm 2nd\ fr} \begin{bmatrix} x(L) \\ x'(L) \\ y(L) \\ y'(L) \end{bmatrix} \tag{20}$$

with

$$M_{\rm 2nd\ fr} = \begin{bmatrix} 1 & 0 & 0 & 0 \\ 0 & 1 & -\frac{C_M}{2}\sqrt{\frac{1+x'^{\,2}(L)+y'^{\,2}(L)}{\gamma^2(L)-1}} & 0 \\ 0 & 0 & 1 & 0 \\ \frac{C_M}{2}\sqrt{\frac{1+x'^{\,2}(L)+y'^{\,2}(L)}{\gamma(L)^2-1}} & 0 & 0 & 1 \end{bmatrix}. \tag{21}$$

Note that these transfer maps are not linear as the transverse momenta appear in the transfer matrices. However, when the momenta are small, then these maps are roughly linear, and furthermore, reduce to the maps for a storage ring solenoid if γ is large.

5 Uniform Solenoid Field with Steerings and RF

Now we must determine the maps for beam propagation through the bulk of the section, where the fields are assumed to be uniform. The relevant Newtonian equations of motion are

$$\frac{d(\gamma\dot{x})}{dt} = \frac{q}{m_e}\left(\dot{y}B_s - \dot{s}B_y\right) \tag{22}$$

and

$$\frac{d(\gamma\dot{y})}{dt} = \frac{q}{m_e}\left(\dot{s}B_x - \dot{x}B_s\right). \tag{23}$$

Extensive integration, differentiation, and substitution using these two equations produces an equation of motion for x and one for y. The equation for x is

$$\begin{aligned} 0 \;=\; & \gamma^2\frac{d^2x}{d\gamma^2} + \gamma\frac{dx}{d\gamma} + \left(\frac{C_M}{C_E}\right)^2 x + \frac{q}{m_e c\, C_E^2}\left(B_y - \frac{B_x C_M}{C_E}\right)\gamma \\ & + \frac{C_M}{C_E^2}\left[\frac{qB_x\gamma(s(0))}{m_e c\, C_E} - C_M x(s(0)) - \gamma(s(0))\, y'(s(0))\right] \end{aligned} \tag{24}$$

where it was assumed that the particle energy was high in certain steps so that the solution would be tractable. The solution is found from *Mathematica* [4] and the following definitions:

$$S_R \equiv \sin\left(\frac{C_M}{C_E}\ln\left(\frac{\gamma_L}{\gamma_0}\right)\right) \tag{25}$$

$$C_R \equiv \cos\left(\frac{C_M}{C_E}\ln\left(\frac{\gamma_L}{\gamma_0}\right)\right). \tag{26}$$

The solution for x after a length $s = L$ is

$$\begin{aligned} x_L &= \frac{qB_x\left[\gamma_0\left[(C_R-1)\frac{C_E}{C_M}-S_R\right]+C_M L\right]+qB_y\left[\gamma_0\left(C_R+\frac{C_E S_R}{C_M}\right)-\gamma_L\right]}{m_e c\,(C_E^2+C_M^2)} \\ &\quad + x_0 + \frac{x_0'\gamma_0 S_R}{C_M} + \frac{y_0'\gamma_0(1-C_R)}{C_M} \end{aligned} \tag{27}$$

while the value of x' is

$$\begin{aligned} x_L' &= \frac{qB_x\left[C_M-\frac{\gamma_0}{\gamma_L}(C_E S_R+C_M C_R)\right]+qB_y\left[\frac{\gamma_0}{\gamma_L}\left(C_E C_R-C_M S_R\right)-C_E\right]}{m_e c\,(C_E^2+C_M^2)} \\ &\quad + \frac{x_0'\gamma_0 C_R}{\gamma_L} + \frac{y_0'\gamma_0 S_R}{\gamma_L}. \end{aligned} \tag{28}$$

If there are no steerings, i.e. if $B_x = B_y = 0$, then the transfer map for the interior of the RF cavity-solenoid is linear in the transverse coordinates. In general though, there are steerings, and we then have the affine map

$$\begin{bmatrix} x_L \\ x_L' \\ y_L \\ y_L' \end{bmatrix} = M_{\mathrm{cav-sol}} \begin{bmatrix} x_0 \\ x_0' \\ y_0 \\ y_0' \end{bmatrix} + M_{\mathrm{steer}} \tag{29}$$

where

$$M_{\mathrm{cav-sol}} = \begin{bmatrix} 1 & \frac{\gamma_0 S_R}{C_M} & 0 & \frac{\gamma_0(1-C_R)}{C_M} \\ 0 & \frac{\gamma_0 C_R}{\gamma_L} & 0 & \frac{\gamma_0 S_R}{\gamma_L} \\ 0 & -\frac{\gamma_0(1-C_R)}{C_M} & 1 & \frac{\gamma_0 S_R}{C_M} \\ 0 & -\frac{\gamma_0 S_R}{\gamma_L} & 0 & \frac{\gamma_0 C_R}{\gamma_L} \end{bmatrix} \tag{30}$$

and

$$\begin{aligned} M_{\mathrm{steer}} &= \begin{bmatrix} \gamma_0\left[(C_R-1)\frac{C_E}{C_M}-S_R\right]+C_M L & \gamma_0\left(C_R+\frac{C_E}{C_M}S_R\right)-\gamma_L \\ C_M-\frac{\gamma_0}{\gamma_L}(C_E S_R+C_M C_R) & \frac{\gamma_0}{\gamma_L}\left(C_E C_R-C_M S_R\right)-C_E \\ -\gamma_0\left(C_R+\frac{C_E}{C_M}S_R\right)+\gamma_L & \gamma_0\left[(C_R-1)\frac{C_E}{C_M}-S_R\right]+C_M L \\ -\frac{\gamma_0}{\gamma_L}\left(C_E C_R-C_M S_R\right)+C_E & C_M-\frac{\gamma_0}{\gamma_L}(C_E S_R+C_M C_R) \end{bmatrix} \\ &\quad \times \begin{bmatrix} B_x \\ B_y \end{bmatrix} \frac{q}{m_e c\,(C_E^2+C_M^2)}. \end{aligned} \tag{31}$$

Note that the steerings constitute the additive matrix M_{steer}, but do *not* affect the linear matrix $M_{\mathrm{cav-sol}}$. This matrix is affected only by the longitudinal magnetic and electric fields.

6 The Complete Map

The transfer map for the cavity-solenoid consists of first applying the map from Equation 18 for the first fringe, then using the map from Equation 29 as many times as necessary, and finally using Equation 20 for the second fringe.

Any given set of steerings may not extend the entire length of the cavity-solenoid. Therefore, the interior of the section may require several applications of Equation 29. For example, if there are two sets of steering coils around a section, then there would be one application for each steering set (two applications) and one application for each segment without steerings (three more applications) for a total of five applications of Equation 29. The positions $s = 0$ and $s = L$ would apply to the ends of each *segment* of the cavity-solenoid element.

Between each application of the transfer maps for transverse motion, it is also necessary to calculate the new energy from Equation 4.

Because of the dependence of the nonlinearities in the longitudinal displacement formula and the presence of the energy in so many terms in the linear transfer matrices, it is impossible to create a general 6×6 transfer matrix.

7 Focal Length of Cavity-Solenoid

A focal length f can be defined for the cavity-solenoid if there are no steerings. The focal length is defined as the distance after the end of the solenoid that a beam will cross the axis assuming the beam entered the section with no transverse momentum. The transverse coordinate vector of a particle before the section is $[x_b, 0, 0, 0]$. After leaving the ending fringe field, the particle coordinates will be

$$\begin{bmatrix} x_a \\ x'_a \\ y_a \\ y'_a \end{bmatrix} = \begin{bmatrix} 1 + C_R \\ -\frac{C_M S_R}{2\gamma_L} \\ -S_R \\ \frac{C_M(1-C_R)}{2\gamma_L} \end{bmatrix} \frac{x_b}{2}. \tag{32}$$

The focal length can be shown to be

$$f = \frac{2\gamma_L(1 + C_R)}{C_M S_R}. \tag{33}$$

8 RF Cavity-Solenoid as other Elements

If certain fields of the cavity-solenoid are off, then it may behave like other, regular accelerator components. The zero-field limits of the transfer maps do recreate the maps of the other components.

With no RF, V and E are 0. If the steerings are also off, then the cavity-solenoid map is identical to a solenoid map. It helps to notice that the normally-encountered solenoid strength is $k_s = C_M/\gamma$. If the solenoid is much shorter than one cyclotron period length, then the focal length in Equation 33 reduces to the usual result of

$$f = \frac{4}{k_s^2 L}. \tag{34}$$

If the RF is on, but the solenoid and steerings are off, then we have the map of an RF cavity alone. If the RF and solenoid are off, but the steerings are on, then the cavity-solenoid behaves like a magnetic kicker. If no fields exist, then the transfer maps become that of a drift space.

The RF cavity-solenoid with steerings has been incorporated into *BMAD* as a new element called "accel_sol." The low-field limits have been used to check that the cavity-solenoid reproduces the aforementioned, regular elements.

9 Actual Length of Solenoid Fringe Field

It was assumed in Section 4 that the fringe field was infinitesimally thin. In reality, there is a considerable distance over which the solenoid field rises to (or falls from) its maximum value. Consider the following schematic of a solenoid:

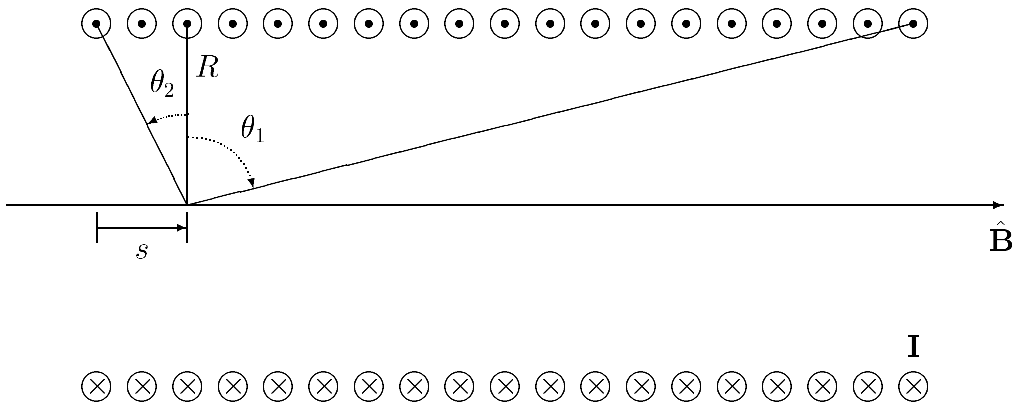

Figure 1: Lengthwise cross section of a solenoid of radius R. The direction of the field along the axis is shown. The angle θ_1 is negative as shown. The distance s is from the end of the solenoid to the point where the field is measured (along the axis).

The field along the axis at position s is determined from the Biot-Savart law [5]:

$$B_s = \frac{\mu_0 n I}{2}(\sin(\theta_2) - \sin(\theta_1)). \tag{35}$$

If we consider a very long solenoid, then we may easily find what longitudinal distance is required for the field to change by the "middle" fraction f of its maximum value. Algebraically, the distance expressed as a number of solenoid radius lengths is

$$\frac{2s}{R} = \frac{2}{\sqrt{f^{-2} - 1}}. \tag{36}$$

Graphically, Equation 36 is shown in Figure 2.

As an example, the distance required for the field to increase by the middle fraction 0.9, i.e. from 5% to 95% of its maximum value, is seen to be about the distance of four radii. Half of this distance (one diameter) is outside of the solenoid.

In the CESR linac, there are a few places where the solenoid fringe field significantly overlaps neighboring elements. An overlap implies that treating sequential elements as disjoint optics is not entirely correct. Nevertheless, it would be difficult to superimpose an arbitrary fringe onto a neighboring element. Because the true solenoid field is longer than the simulated field, more positrons are probably captured in the linac than is indicated by the simulation.

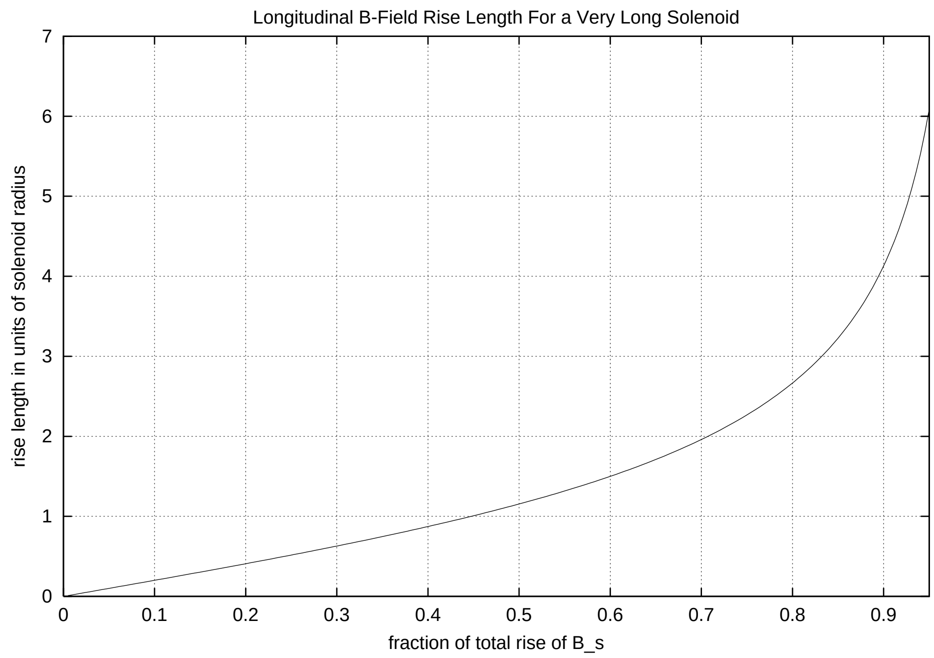

Figure 2: Total longitudinal distance required (centered at one end of the solenoid) for the magnetic field on the axis to change by a fraction of its maximum value at the center of the solenoid. The right edge of the plot shows the length for 95% of the field rise.

References

[1] *BMAD* lattice program, maintained by David Sagan, Laboratory of Nuclear Studies, Cornell University.

[2] Daniel Bret Fromowitz, Ph.D. Dissertation, not yet completed.

[3] Martin Reiser, *Theory and Design of Charged Particle Beams*, John Wiley & Sons, Inc., New York, 1994.

[4] Wolfram Research, Inc., *Mathematica* Version 2.2 for the X Window System, Champaign, Illinois, 1993.

[5] Raymond A. Serway, *Physics For Scientists and Engineers*, Saunders College Publishing, Philadelphia, 1990.